Characterization of the ITER CS conductor and projection to the ITER CS performance

N. Martovetsky^a, T. Isono^b, D. Bessette^c, A. Devred^c, Y. Nabara^b, R. Zanino^d, L. Savoldi^d, R. Bonifetto^d, P. Bruzzone^e, M. Breschi^f, and L. Zani^g

^aUS ITER Project Office, 1055 Commerce Park Dr., Oak Ridge, TN 37831, USA and
Lawrence Livermore National Laboratory, Livermore, CA 94550, USA

^bNational Institutes for Quantum and Radiological Science and Technology(QST), 801-1 Mukoyama, Naka-shi, Ibaraki-ken 311-0193 JAPAN

^cITER Organization, Route de Vinon sur Verdon, CS 90 046, 13067 St Paul lez Durance Cedex, France

^dPolitecnico di Torino corso Duca degli Abruzzi 24, 10129 Torino ITALY

^eSwiss Plasma Center CH 5232 - Villigen PSI Switzerland

^fUniversity of Bologna Viale Risorgimento 2, 40136, Bologna, Italy

^gCEA Cadarache. 13108 St Paul lez Durance Cedex. France

The ITER Central Solenoid (CS) is one of the critical elements of the machine. The CS conductor went through an intense optimization and qualification program, which included characterization of the strands, a conductor straight short sample testing in the SULTAN facility at the Swiss Plasma Center (SPC), Villigen, Switzerland, and a single-layer CS Insert coil recently tested in the Central Solenoid Model Coil (CSMC) facility in QST-Naka, Japan. We obtained valuable data in a wide range of the parameters (current, magnetic field, temperature, and strain), which allowed a credible characterization of the CS conductor in different conditions. Using this characterization, we will make a projection to the performance of the CS in the ITER reference scenario.

Keywords: Superconducting magnets, voltage measurement, strain measurement, degradation, and performance

1. Introduction

A Central Solenoid Insert (CSI) was tested in 2015, [1] in the background field of the Central Solenoid Model Coil (CSMC).

The CSI design, analysis, and fabrication are given in [2] and [3]. The test showed that the CSI had no degradation because of the cyclic electromagnetic (EM) loading or cooldown-warm up cycles. The CSI showed losses in line with expectations from the tests at SULTAN or at the University of Twente, including significant reduction of losses because of cycling.

One of the main goals of the CSI tests was to characterize the conductor behavior to compare its performance with SULTAN measurements and to create a predictive model for ITER CS performance. The details of the conductor design are given in [4],[5].

2. Analysis approach

To characterize the CS conductor, we will use a strand correlation of the critical current vs. strain, magnetic field and temperature $I_c\left(e,\,B,\,T\right)$ measured at the University of Twente.

The formula for the correlation is described in [6] and parameters of the correlation for the CSI conductor are given in Table 1.

We are trying to describe performance of the conductor using a simplified model. It is well known that the strain in the 900-strand conductor has a very

complex spatial distribution [7]. Also, the strain comes from different sources. The superconductor is formed during heat treatment at 650 °C, and during the cooldown to room temperature and then to the supercritical helium temperature of about 4.5K, it produces a cooldown strain, which is usually compressive and is near -0.5% to-0.7% for cable in conduit conductor (CICC) in a steel jacket.

Table 1. Correlation parameters of the CSI strand

Parameter	Value
C _{a1}	45.74
C_{a2}	4.431
e_{0a}	0.00232
e_{m}	-0.00061
$\mathrm{Bc}_{20\mathrm{m}}$	29.39
T_{c0m}	16.48
C_1	21851
p	0.556
q	1.698

When the coil is energized, the EM force produces a hoop tensile strain and a lateral compressive force that crushes the cable against the wall of the jacket. Both strains are proportional to the product of IxB.

To find T_{cs} and the effective strain, we used integrated electrical field over the cable cross section considering the real transition to normal state with N=7.

$$E = E_c \int_{S} \left(\frac{j}{j_c(T, B, \varepsilon)} \right)^N \frac{dS}{S} = E(Beff)$$
 (1)

Here E_c is 10 mV/m, and N is the fitting parameter, $j_c(T,B,\varepsilon)$ is the strand current characterization and B_{eff} is the effective field, which is higher than the average magnetic field in the cable cross section, S is the cross section. The electric field in the conductor in SULTAN and in CSI was calculated in the same way using integration (1).

That was done to consider the varying magnetic field in the cross section. The temperature, current and strain distribution were assumed to be uniform in the cross section. Usually the hoop strain improves performance and increases T_{cs} , while lateral crushing force reduces T_{cs} due to the high sensitivity of the Nb₃Sn to the lateral compressive stress and bending of the strands. We, however, are trying to describe the strain in the cable with one number – "effective total strain", which will have these three components of the strain – cooldown, longitudinal (hoop), and lateral crushing:

$$\mathcal{E}_{total} = \mathcal{E}_{cd} + \mathcal{E}_{hoop} + \mathcal{E}_{crush} \tag{2}$$

The hoop and crushing stress are both proportional to IxB. We assume that a simple addition adequately reflects the effect of these components on describing the performance of the CS conductor.

We could not directly measure the cooldown strain, but we can deduce this strain by extrapolating the total strain to conditions of zero EM force.

We cannot directly measure the strain in the cable for obvious reasons. However, we did measure the strain in the jacket. We know from experience that strain in the jacket is not necessarily equal to the strain in the cable. However, we expect that the strain in the cable will be relatively close to and proportional to the jacket strain. We will calculate the cable strain by fitting the measured T_{cs} and then we will find a correlation with measured jacket strain.

We equipped the CSI with several strain gauges to measure the hoop strain in the CS conductor jacket.

We will use CSI data along with the data from SULTAN on the conductor that went into the CSI to compare the crushing strain in two conductors.

Knowing the strain in the jacket, and by constructing a correlation between the hoop strain in the jacket and the current sharing temperature of the CS conductor, we should be able to predict the temperature margin in the ITER CS, which has approximately the same crushing force as in the CSI but a significantly higher hoop strain in the conductor.

3. CSI instrumentation

The ability to instrument the CSI gave a unique opportunity to obtain conductor data that were not available otherwise. The CSI instrumentation schematic is shown in Fig. 1. We had seven strain gauges bonded to the conductor jacket to monitor strain in the jacket.

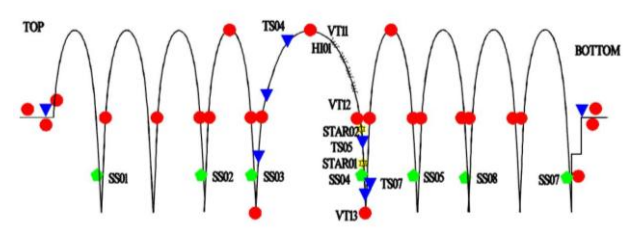


Fig. 1. Instrumentation in CSI. Circles – voltage taps, trianglestemperature sensors, pentagons – strain gauges.

We measured the electrical field in the conductor using voltage taps, and we measured the temperature in the conductor. We also calculated the magnetic field distribution. All this information allowed us to build a correlation of the "effective strain" in the CS conductor, using strand correlation $I_c(e, B, T)$ that was measured by University of Twente group.

4. Strain measurements in CSI

We had strain measurements on all the runs during the CSI campaign. The measurements in the beginning of the campaign were not reliable due to the signal conditioners malfunctioning. After replacing the conditioners, which took place after the first warmupcooldown cycle, the data became very stable.

The most instrumented area in the middle of the coil that develops the v however, no hoop strain voltage first is represented by the strain gauge SS04. During the CSI test campaign the CSI currents ranged from -50 kA to 60 kA and the peak field was up to 13 T. Thus, the hoop strain changed the sign from compressive in the "reverse" charging mode to the usual tensile strain when the field generated by CSMC and CSI were in the same direction.

The strain is remarkably linear with the electromagnetic force, as expected, and crosses the strain line very close to zero (shown in Fig. 5 along with the cable strain and discussion). That completes characterization of the jacket strain vs. IxB parameter.

If the turns would support the hoop forces only by tension in the jacket, the hoop strain could be expressed as:

$$\varepsilon_{hoop} = \frac{IBR}{ES} \tag{3}$$

where I is the transport current, B is the average field in the cable cross section, R is the mean radius of the turn, S is the jacket cross section, and E is the Young modulus of the jacket. In our case, the CSI turns are spread with G-10 spacers in between per [2], which carry a significant load, so the strain in the jacket is lower. Comparing the strain from equation (3) with the ones that we measured, we found that only 62% of the strain calculated from (2) was measured in the jacket. This agrees with the ANSYS model [1].

5. Strain assessment in SULTAN tests

The strain in the SULTAN sample, CSJA6, that has the same conductor as the CSI (left leg) and identical to it with slightly longer twist pitch (right leg), can be deduced from the T_{cs} measurements, shown in Table 2.

Fig.2 shows T_{cs} evolution versus cycles both for SULTAN sample and for CSI. The T_{cs} in CSI is higher due to higher hoop strain. Warm up-cooldown cycles were applied at 5000, 8000 and 10000 cycles.

SULTAN tests have only cooldown strain and crushing strain; however, no hoop strain. During testing, the T_{cs} is improved until saturation after 10000 cycles and therefore we process only the data after stabilization. In the CSI, the improvement of the T_{cs} is much less pronounced but, again, we process the T_{cs} obtained towards the end of the campaign.

Effective strain vs. IxB crushing force in SULTAN is shown in Fig. 3 for both legs.

The T_{cs} data, which were used for assessment of strain, are given in Table 2, which are taken from [8].

Table 2. T_{cs} results from SULTAN tests of the CSJA6

B, T	I, kA	T _{cs} , Right, K	T _{cs} , Left, K
10.85	45.1	7.20	7.28
10.85	40	7.47	7.53
10.4	40	7.77	7.84
9.95	40	8.11	8.18
10.85	30	7.99	8.04
10.4	30	8.30	8.34

It correlates reasonably well with the lateral crushing force IxB and extension of the trend to the zero IxB parameter suggests the effective cooldown strain of -0.61%. The crushing strain coefficient for the right leg is:

$$\varepsilon_{crush} = 1.27 * 10^{-6} * IxB[kAT] \tag{4a}$$

For the left leg, it is:

$$\varepsilon_{crush} = 1.05 * 10^{-6} * IxB[kAT] \tag{4b}$$

6. Strain assessment in the CSI

Fig. 4 shows assessment of the effective strain in the CSI in both modes of operation – direct charge, when the CSI and CSMC field directions coincide and in the reverse charge mode, when the currents are opposite. In the last case CSI is compressed in hoop direction by the CSMC magnetic field. Although the vector of force changes its direction, we speculate that behavior of the CSI conductor does not depend on the crushing force direction, only on the value. The T_{cs} performance, however, is very sensitive to the direction of the hoop strain.

The effective strain shown in Fig. 4 gives some interesting observations. Extension of the strain to the zero IxB from the direct charge suggests cooldown strain is negative -0.59%. Extension of the strain line to zero IxB from the reverse charge data points at -0.584%, which is a good agreement, although a little lower than -0.61% that was observed in SULTAN measurements, see trend line approximations in Fig. 3.

The remarkable part of Fig. 4 is that in direct charge, the hoop strain in the cable and the crushing strain balance each other almost ideally. In the reverse charge part, the crushing strain and the hoop strain combine to

reduce T_{cs} , which gives the following dependence vs. IxB in CSI:

$$\varepsilon_{cd} = -0.59\%$$

$$\varepsilon_{hoopcable} = 1.25 * 10^{-6} IB = \alpha \varepsilon_{hoopjacket}$$

$$\varepsilon_{crush} = -1.25 * 10^{-6} IB$$

$$8$$

$$7.8$$

$$7.6$$

$$7.4$$

$$4$$

$$7.2$$

$$7$$

$$6.8$$

$$6.6$$

$$6.4$$

$$CSJA6 Left leg$$

$$CSJA6 Right leg$$

$$CSJA6 Right leg$$

Fig. 2. T_{cs} evolution in CSI and SULTAN CSJA6 at comparable conditions

10000

Cycles

15000

20000

5000

6.2 + 6 + 0

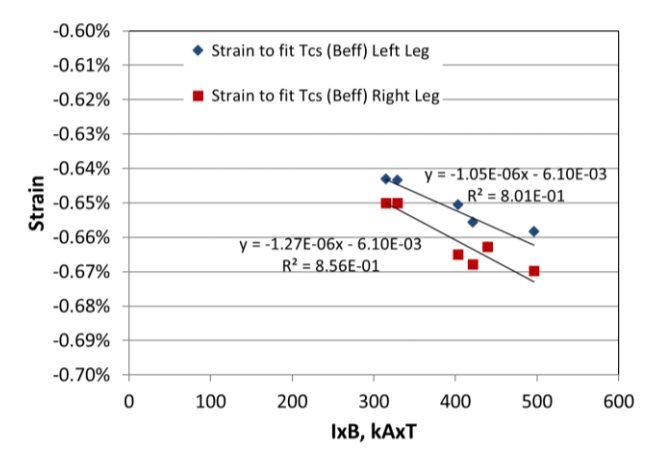


Fig.3. Effective total strain in the CSJA6 SULTAN tests

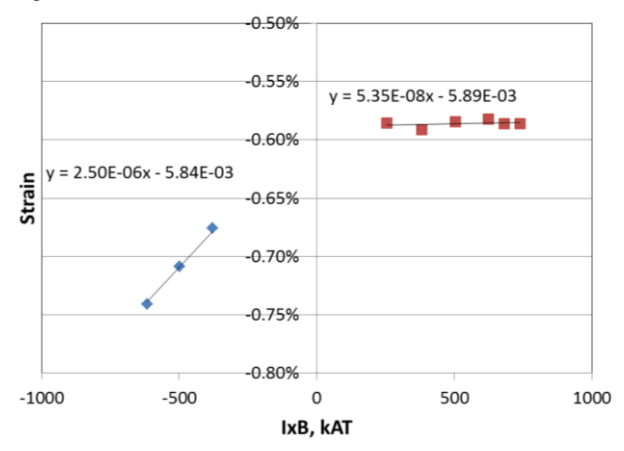


Fig. 4. Effective total strain in CSI deduced from Tcs measurements

where the current I is expressed in [kA] and B is expressed in [T], α is the correlation coefficient between strain in the cable and strain in the jacket.

It is desirable to express the hoop strain in the cable as a function of strain in the jacket, since our dependence of the hoop strain vs. parameter IxB is only good for the CSI, while the crushing strain is supposed to be a universal for the conductor.

Fig. 5 shows comparison of the measured hoop strain in the jacket vs. deduced hoop strain in the cable. As we can see, the hoop strain in the cable represents about 85% of the jacket, thus we can express the correlation between the hoop strain in the cable and in the jacket as:

$$\varepsilon_{hoopcable} = 0.85 \varepsilon_{hoopjackel}$$
 (6)

It is interesting to compare the crushing force dependence vs. IxB in SULTAN and CSI. Fig. 6 gives such a comparison for both SULTAN legs, described in **Error! Reference source not found.** as conductors B and C, which shows a very similar pattern. Note, that the left leg, which was cut from the CSI conductor, showed slightly different slope than the right leg, which is the identical conductor but taken from a different length. This is an indication of the scatter in performance of the CS conductor.

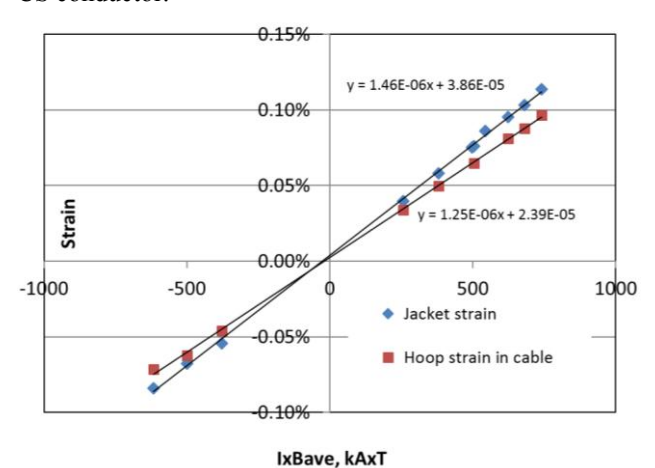


Fig. 5. Hoop strain in the jacket vs hoop strain in the cable in CSI tests.

7. Projection of CS conductor behavior in the ITER CS

With the established correlations of the crushing and hoop strains, we now can project the current sharing temperature in the ITER CS in the most stringent condition, which is the Initial Magnetization (IM) right before the plasma initiation.

Peak average longitudinal strain in the CS jacket in the CS at IM (0.19%), effective field (B = 12.6 T) and current (40 kA) are known [9], the effective strain in the cable will be:

$$\varepsilon_{total} = -0.59\% + 0.19\% * 0.85 - 1.25*10^{-6}*40*12.6 = -0.49\%$$
 (7)

Thus, the effective strain in the CS will be improved by 0.1% in comparison with CSI. That reduction in the compressive strain should give about 0.6 K additional temperature margin at IM to T_{cs} =7.35 K in comparison with the CSI data at IM conditions because the hoop strain in the CS is significantly higher than in the CSI, while the crushing force is the same.

The original acceptance criterion for CS $T_{cs}\, at \,\, IM$ is 5.2 K.

At the End of Burn conditions in ITER operation, the hoop EM strain in the ITER CS jacket will be 0.176% in comparison with the CSI, where we measured 0.086% [9].

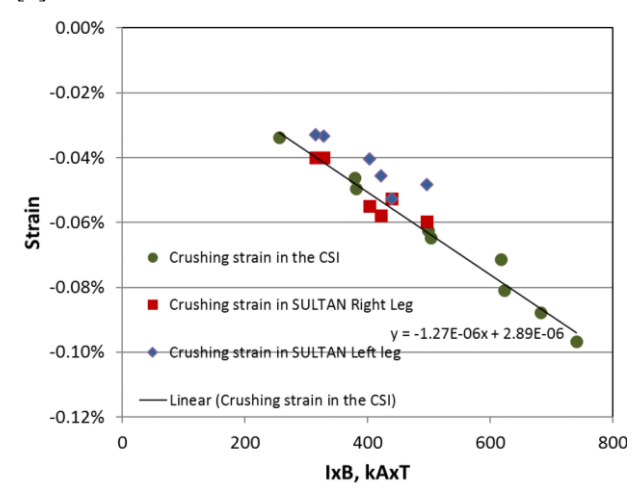


Fig. 6. Crushing strain in CSI and SULTAN, the line is the CSI trend line

This increase of the hoop strain will result in increase of the T_{cs} parameter by 0.6 K from 6.97 K measured in the CSI to 7.57 K. This is a very significant increase in temperature margin of the CS magnet that improves reliability and robustness of the machine.

8. Conclusions

The SULTAN and CSI test data demonstrated again sensitivity of the large CICC with Nb₃Sn strands to the strains. Using test data and a simplified model we characterized the conductor behavior in terms of three components of the strain – cooldown, longitudinal and lateral crushing strains. We see that effect of the crushing force on the performance of the conductor is similar in the straight sample in SULTAN tests and in a solenoid of CSI. The hoop strain effect predicts that ITER CS will have an additional significant margin, which gives an additional assurance in CS successful operation.

9. Acknowledgements

This manuscript has been authored by UT-Battelle, LLC under U.S. Department of Energy Contract No. DE-AC05-00OR22725 and LLNL under DOE Contract No. DE-AC52-07NA27344. The United States Government retains and the publisher, by accepting the article for publication, acknowledges that the United States Government retains a non-exclusive, paid-up, irrevocable, world-wide license to publish or reproduce the published form of this manuscript, or allow others to do so, for United States Government purposes.

The views and opinions expressed herein do not necessarily reflect those of the ITER Organization.

References

- [1] N. Martovetsky, T. Isono, D. Bessette et al, "ITER Central Solenoid Insert Test Results", *IEEE Trans. Appl. Supercond.*, vol. 26, no. 4, June 2016, p. 4200605
- [2] A. E. Khodak, N. N. Martovetsky, A. V. Smirnov, P. H.

- Titus, "Optimization of ITER Central Solenoid Insert design", *Fusion Engineering and Design, Volume 88*, Issues 9–10, Oct 2013, pp 1523-1527
- [3] T. Isono, K. Kawano, H. Ozeki et al., "Fabrication of an Insert to Measure Performance of ITER CS Conductor", *IEEE Trans. Appl. Supercond.* vol. 25, no. 3, June 2015 p. 4201004
- [4] D. Bessette, 'Design of a Nb₃Sn cable-in-conduit conductor to withstand the 60,000 electromagnetic cycles of the ITER Central Solenoid', *IEEE Trans. Appl. Supercond.*, vol. 24, no. 3, Jun. 2014
- [5] Y. Nabara, T. Hemmi, H. Kajitani et al, "Impact of Cable Twist Pitch on T_{cs}-Degradation and AC Loss in Nb₃Sn Conductors for ITER Central Solenoids" *IEEE Trans. Appl. Supercond.* vol. 24, no. 3, June 2014 p. 4200705

- [6] L. Bottura and B. Bordini, "*J_c*(*B*,*T*,ε) parameterization of the ITER Nb₃Sn production," *IEEE Trans. Appl. Supercond.*, vol. 19, no. 3, 2009, pp.1521–1524.
- [7] H. Bajas, D. Durville, D. Ciazynski, and A. Devred, "Numerical Simulation of the Mechanical Behavior of ITER Cable-In-Conduit Conductors", *IEEE Trans. Appl. Supercond.*, vol. 20, no. 3, 2010, pp.1467–1470
- [8] Test Report of CSJA6 Conductor Sample in Phases II and III ITER report, ITER_D_PL9C8X v1.1, June 2014
- [9] L. Myatt, DCR for the Qualification of the CS JK2LB Conductor Conduit Helium Inlets and Outlets DCR-1.1.1.1-17-002- V01 - EXPORT CONTROL, US ITER document control center US_D_22NAAA, Nov 2016

Table 1. Correlation parameters of the CSI strand

Parameter	Value
C _{a1}	45.74
C_{a2}	4.431
e_{0a}	0.00232
e_{m}	-0.00061
$\mathrm{Bc}_{20\mathrm{m}}$	29.39
T_{c0m}	16.48
C_1	21851
p	0.556
q	1.698

Table 2. $T_{\rm cs}$ results from SULTAN tests of the CSJA6

B, T	I, kA	T _{cs} , Right, K	T _{cs} , Left, K
10.85	45.1	7.20	7.28
10.85	40	7.47	7.53
10.4	40	7.77	7.84
9.95	40	8.11	8.18
10.85	30	7.99	8.04
10.4	30	8.30	8.34

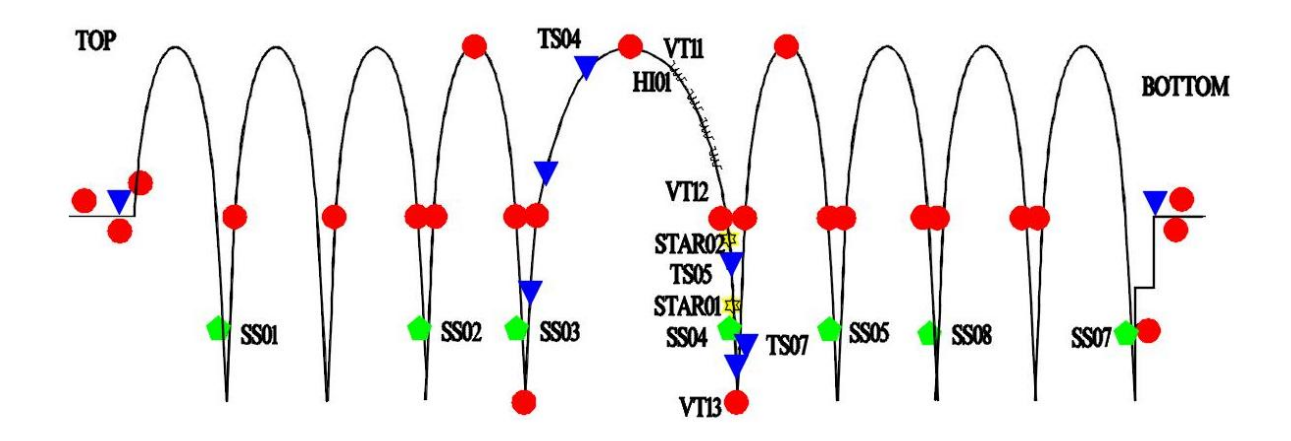


Fig.1

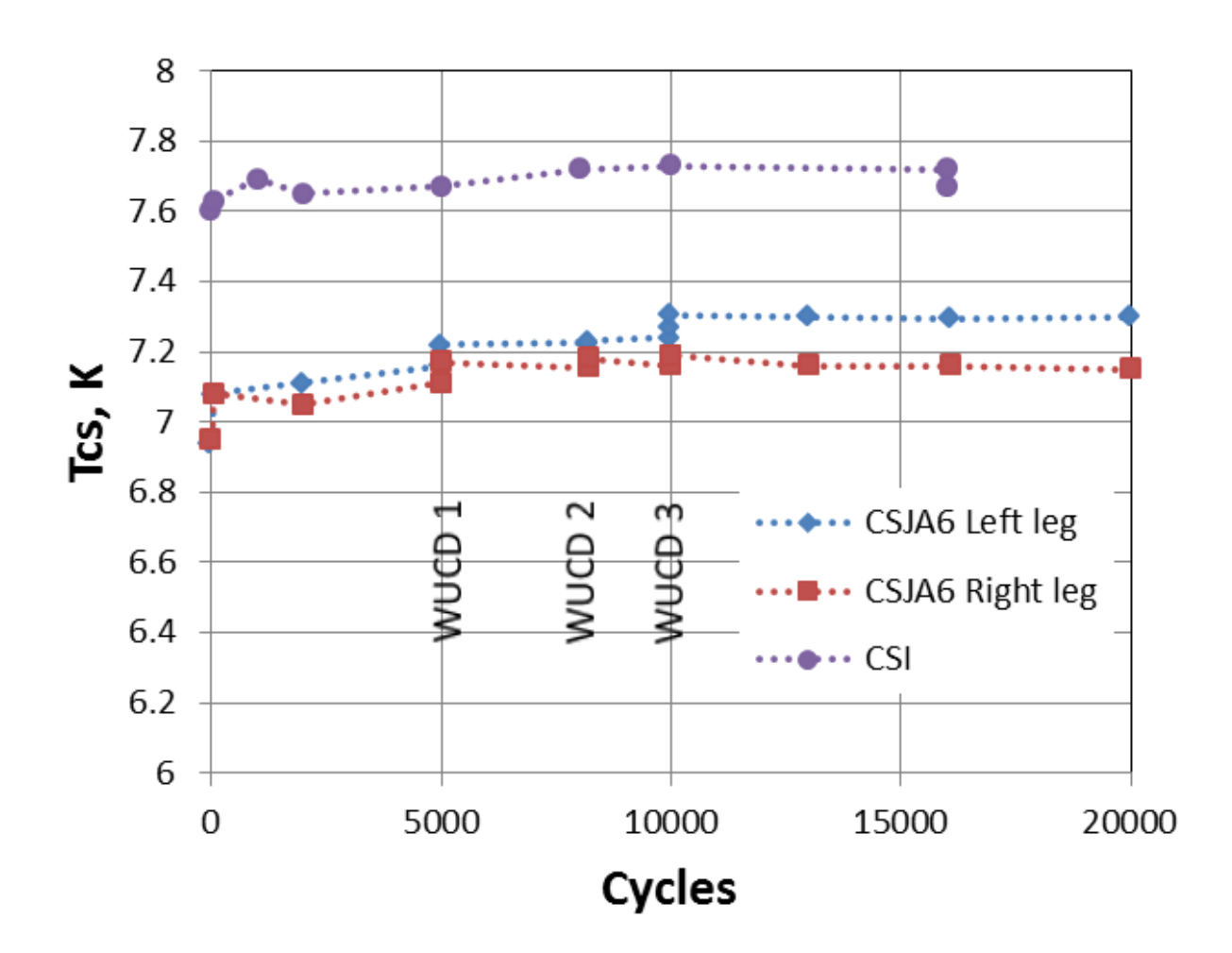


Fig.2

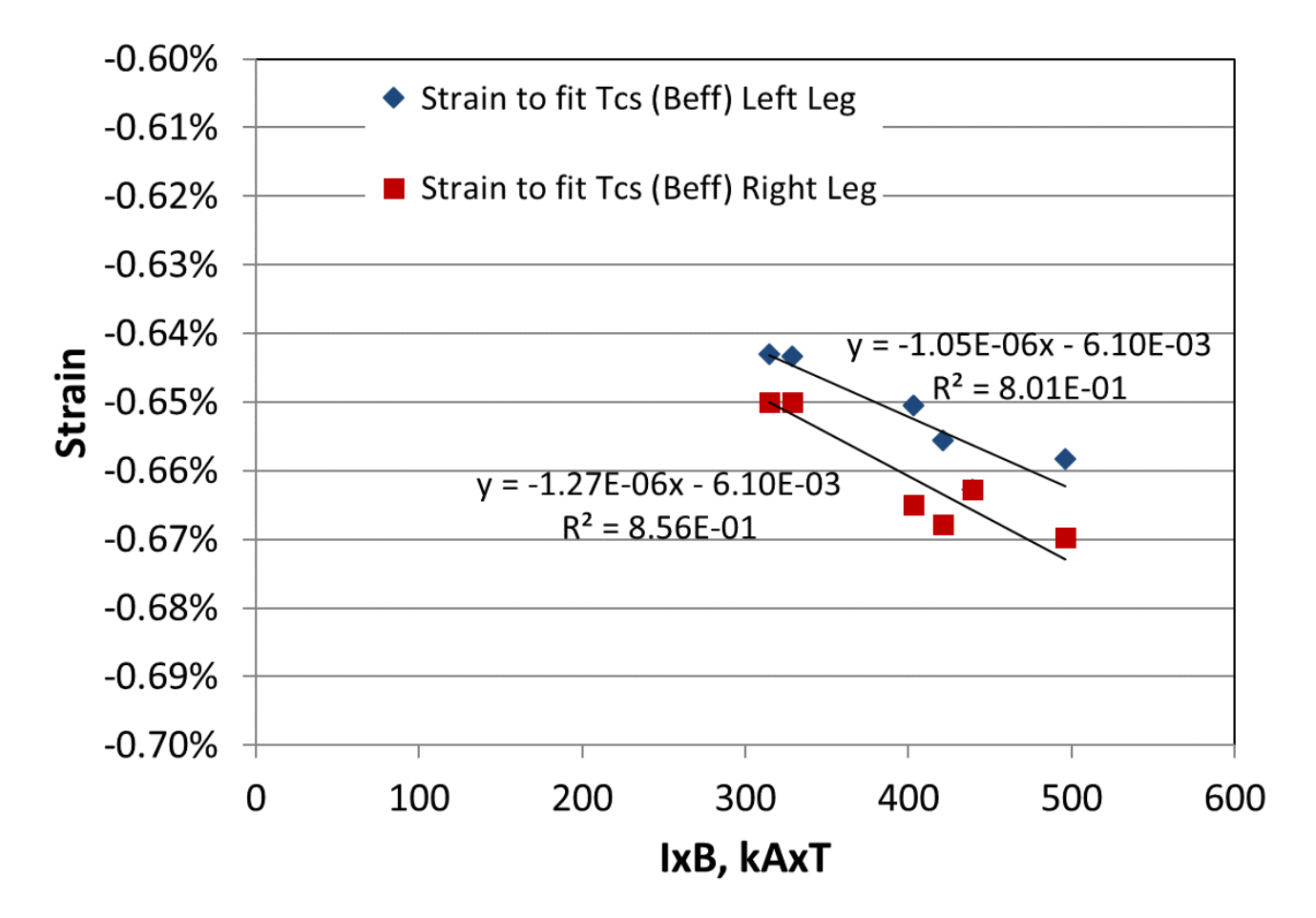


Fig.3

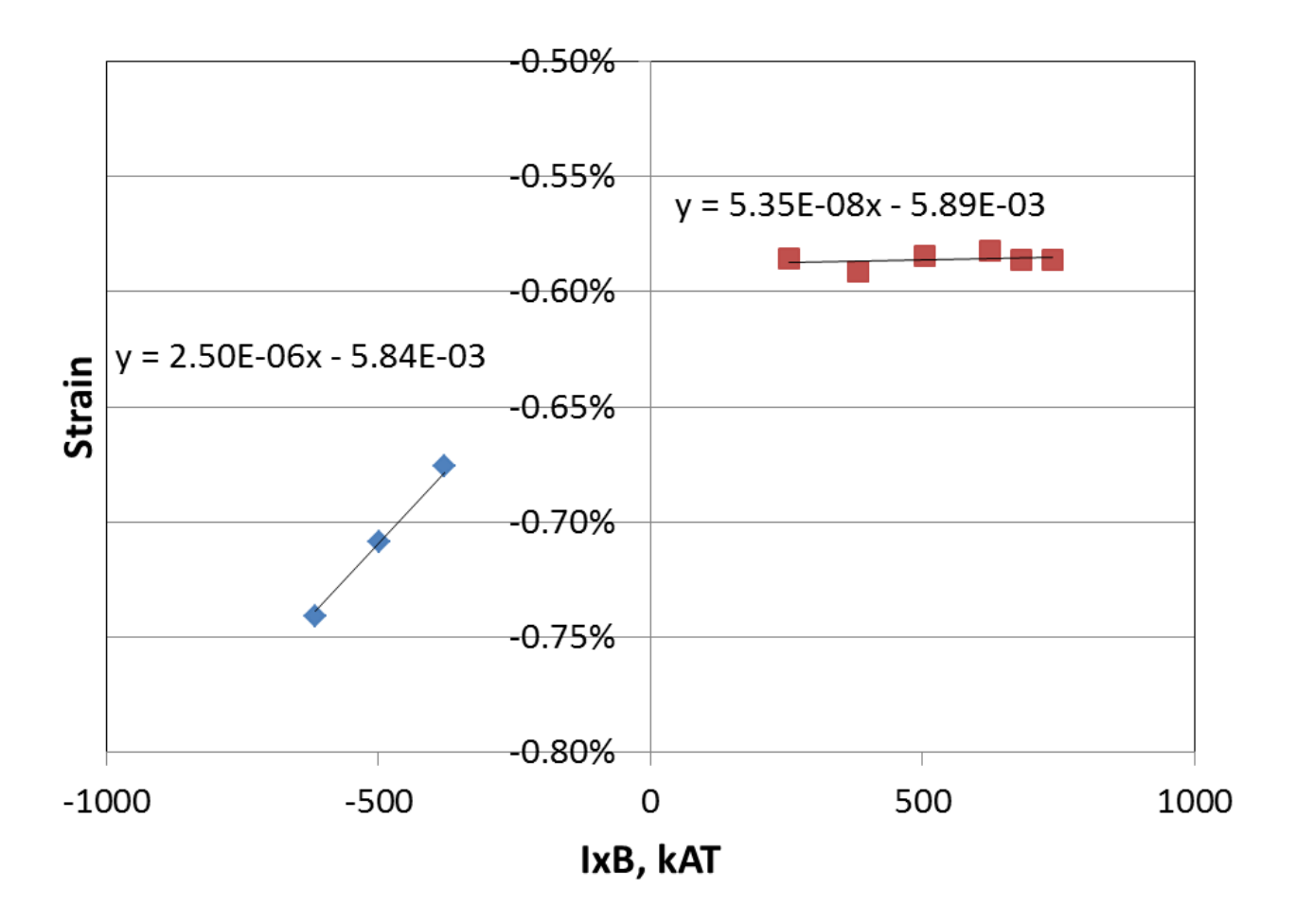
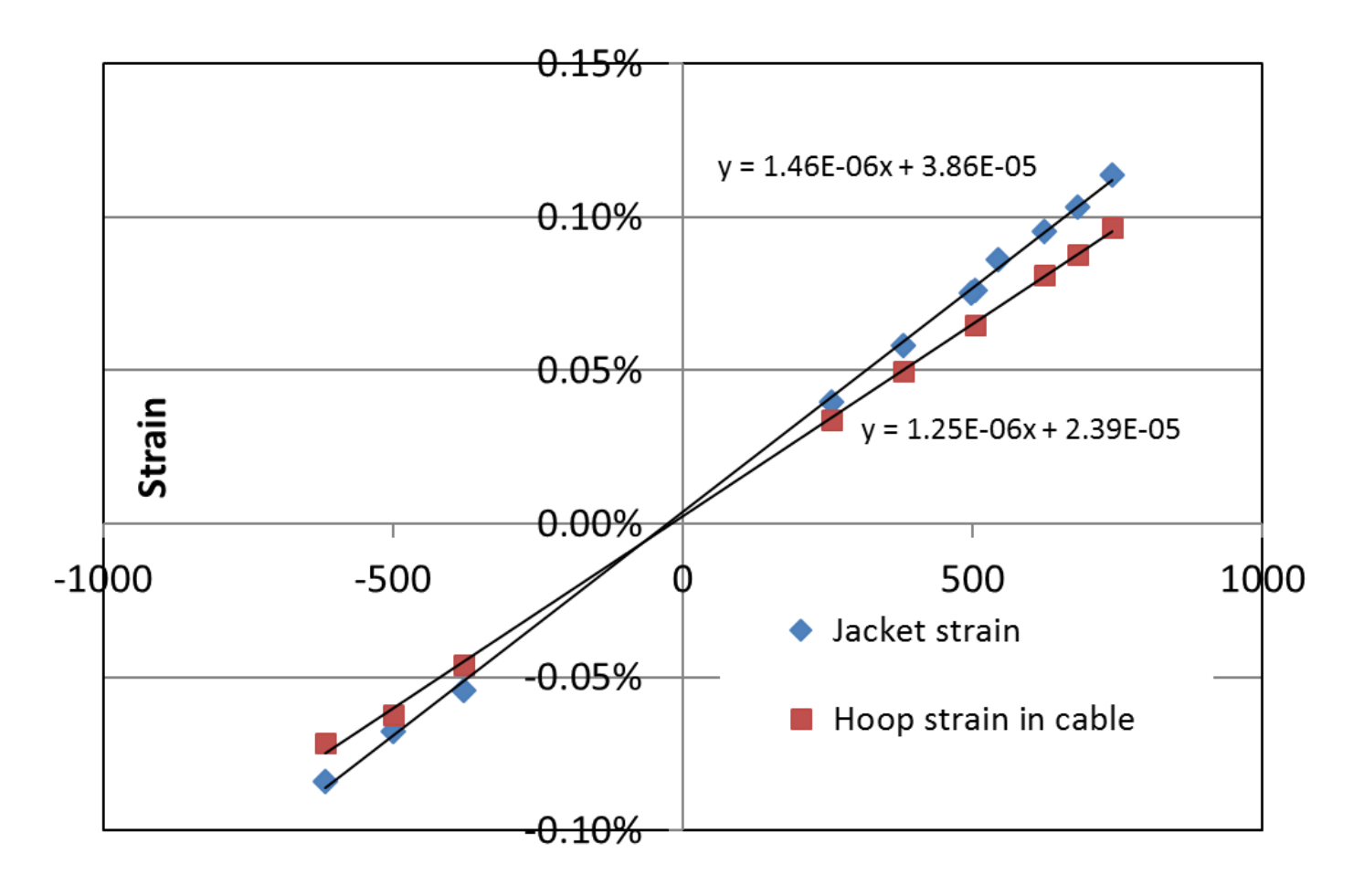


Fig.4



IxBave, kAxT

Fig.5

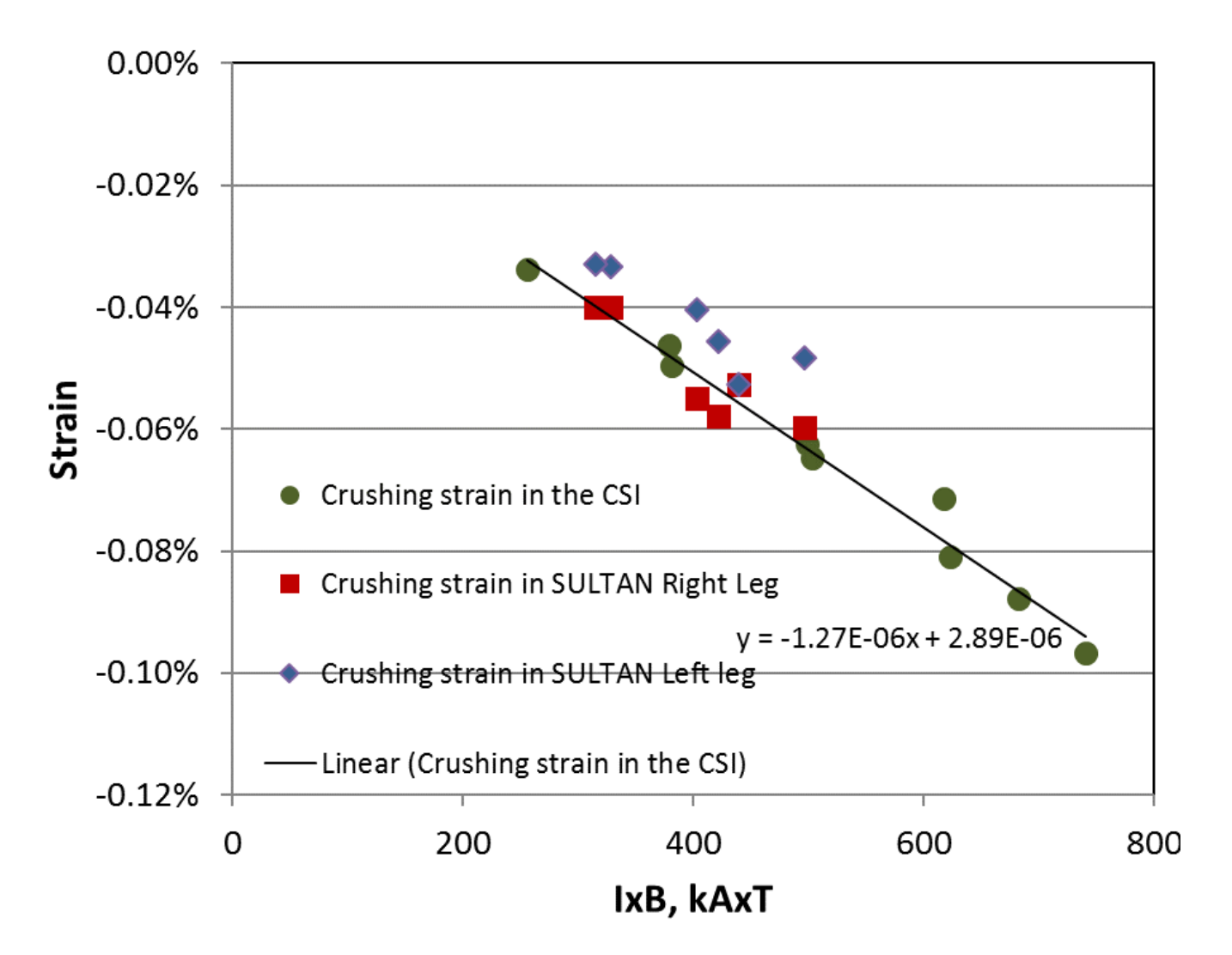


Fig. 6